

Two-dimensional electron gas formed on the indium-adsorbed Si(111) $\sqrt{3}\times\sqrt{3}$ -Au surface

J. K. Kim,¹ K. S. Kim,¹ J. L. McChesney,² E. Rotenberg,² H. N. Hwang,³ C. C. Hwang,³ and H. W. Yeom^{1,*}

¹Center for Atomic Wires and Layers and Institute of Physics and Applied Physics, Yonsei University, Seoul 120-749, Korea

²Advanced Light Source, Lawrence Berkeley National Laboratory, Berkeley, California 94720, USA

³Beamline Research Division, Pohang Accelerator Laboratory, POSTECH, Pohang, Kyungbuk 790-784, Korea

(Received 1 June 2009; revised manuscript received 16 July 2009; published 20 August 2009)

Electronic structure of the In-adsorbed Si(111) $\sqrt{3}\times\sqrt{3}$ -Au surface was investigated by core-level and angle-resolved photoelectron spectroscopy. On the Si(111) $\sqrt{3}\times\sqrt{3}$ -Au surface, In adsorbates were reported to remove the characteristic domain-wall network and produce a very well-ordered $\sqrt{3}\times\sqrt{3}$ surface phase. Detailed band dispersions and Fermi surfaces were mapped for the pristine and In-dosed Si(111) $\sqrt{3}\times\sqrt{3}$ -Au surfaces. After the In adsorption, the surface bands shift toward a higher binding energy, increasing substantially the electron filling of the metallic band along with a significant sharpening of the spectral features. The resulting Fermi surface indicates the formation of a perfect isotropic two-dimensional electron-gas system filled with 0.3 electrons. This band structure agrees well with that expected, in a recent density-functional theory calculation, for the conjugate-honeycomb trimer model of the pristine Si(111) $\sqrt{3}\times\sqrt{3}$ -Au surface. Core-level spectra indicate that In adsorbates interact mostly with Si surface atoms. The possible origins of the electronic structure modification by In adsorbates are discussed. The importance of the domain wall and the indirect role of In adsorbates are emphasized. This system provides an interesting playground for the study of two-dimensional electron gas on solid surfaces.

DOI: 10.1103/PhysRevB.80.075312

PACS number(s): 73.20.Hb, 79.60.Dp

I. INTRODUCTION

Self-assembled metal overlayers on semiconductor surfaces recently attracted considerable interest due to their low-dimensional electronic properties.¹⁻⁴ Metal overlayers on semiconductor surfaces exhibit not only two-dimensional (2D) metallic systems such as Si(111) $\sqrt{3}\times\sqrt{3}$ -Ag,^{5,6} Si(111) $\sqrt{7}\times\sqrt{3}$ -In,⁷ Ge(111) $\sqrt{3}\times\sqrt{3}$ -Sn,⁸ and the dense Pb layers on Si(111),⁹ but also (quasi)one-dimensional (1D) metallic systems such as Si(111)4 \times 1-In (Ref. 10) and Si(111)5 \times 2-Au.^{11,12} On these systems, interesting low-dimensional physics has been discussed such as 2D electron-gas formation,⁵ frustrated 2D Mott insulating ground states,⁸ 1D charge-density-wave phase transition,¹⁰ and 1D band-gap engineering by the adsorbate doping.¹²

Another interesting candidate system for a 2D metal is the Si(111) $\sqrt{3}\times\sqrt{3}$ -Au surface formed by Au adsorbates of around one monolayer (ML).¹³ This surface exhibits a complicated domain-wall structure which depends sensitively on the coverage of adsorbates.¹⁴ The similar domain-wall formation can be found on a few other dense adsorbate systems due to the surface strain such as Pb/Si(111) where the domain wall forms a variety of superstructures with long-range orders.¹⁵⁻¹⁷ Detailed band dispersions and Fermi surfaces of this system were reported recently, which depend systematically on the domain-wall ordering and the concomitant local-structure change.⁹ However, in contrast to Pb/Si(111), a *disordered meandering* domain-wall pattern was observed on the Si(111) $\sqrt{3}\times\sqrt{3}$ -Au surface.^{18,19} The detailed surface ordering was classified according to the domain-wall configuration; the α - $\sqrt{3}\times\sqrt{3}$ phase with the lowest domain-wall density at 0.9 ML of Au, the β - $\sqrt{3}\times\sqrt{3}$ phase with a higher domain-wall density at 1.0 ML, and the 6 \times 6 phase with *ordered* domain walls at 1.1 ML.^{13,20} These domain-wall structures all melt at a higher temperature than 600 °C,

where a domain-wall-free γ - $\sqrt{3}\times\sqrt{3}$ phase is formed.^{14,21}

Throughout this evolution the local $\sqrt{3}\times\sqrt{3}$ structure within the domains and the local structure of domain walls are thought to be preserved.^{13,18,19} However, the detailed atomic structures of the domain and, especially, the domain wall are not fully clear. This is partly due to the existence of the disordered domain-wall structure, which makes the structural analysis by a conventional diffraction technique difficult. As for the $\sqrt{3}\times\sqrt{3}$ domain, it has been widely accepted that the structure is composed of Au and Si trimers, which is similar to the well-established structure of the Si(111) $\sqrt{3}\times\sqrt{3}$ -Ag surface.^{21,22} In detail, three variations of the trimer structure are suggested; twisted trimer (TT),²³ honeycomb trimer (HCT),²⁴ and conjugate-honeycomb trimer (CHCT) (Refs. 25 and 26) models depending on the bond length and the orientation of Au and Si trimers as shown in Figs. 1(a)–1(c).

The electronic structure of the $\sqrt{3}\times\sqrt{3}$ -Au surface depends strongly on the Au coverage and the domain-wall configuration.²⁸ While both α - $\sqrt{3}\times\sqrt{3}$ and β - $\sqrt{3}\times\sqrt{3}$ surfaces have four distinctive surface-state bands consistently, the so-called S1 state near the Fermi level provides an important difference; the α - $\sqrt{3}\times\sqrt{3}$ surface is metallic with the dispersing S1 band in contrast to the β - $\sqrt{3}\times\sqrt{3}$ surface with a flat semiconducting band.²⁸ The 6 \times 6 surface has clearly different, largely dispersionless, bands and is not metallic.²⁸ The origin of such a drastic dependence is unclear.

On the other hand, recently, there was a very interesting report concerning domain walls of the $\sqrt{3}\times\sqrt{3}$ -Au surface. A recent scanning-tunneling microscopy (STM) study²⁷ found that submonolayer In adsorbates on the α - $\sqrt{3}\times\sqrt{3}$ surface eliminate the whole domain wall to yield a very well-ordered and homogeneous $\sqrt{3}\times\sqrt{3}$ (h - $\sqrt{3}\times\sqrt{3}$, hereafter) phase. This phenomenon was explained by the surface-stress relief

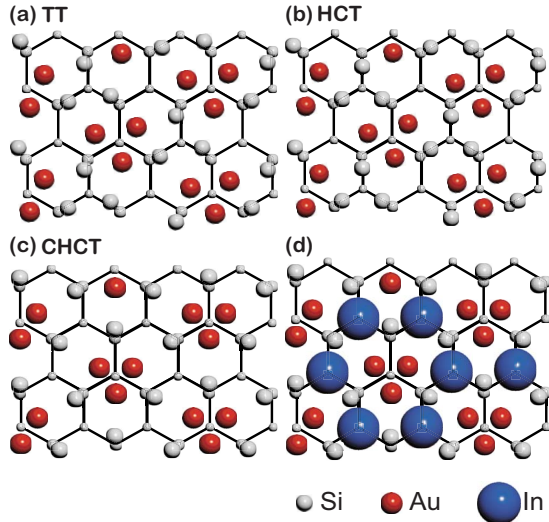


FIG. 1. (Color online) Schematics of the structure models of the $\text{Si}(111)\sqrt{3}\times\sqrt{3}\text{-Au}$ surface; (a) TT, (b) HCT, and (c) CHCT models. (d) The structure model suggested for In adsorbates on the $\text{Si}(111)\sqrt{3}\times\sqrt{3}\text{-Au}$ surface at low temperature. Note that the nominal coverage of this structure is much higher than the experiment (Ref. 27).

caused by the In adsorption but is not trivial at all since the In adsorbates at room temperature (RT) are not imaged by STM and is thus thought to migrate actively on the surface. While the mechanism of the In-induced structural change is interesting enough, we by ourselves are interested in the electronic structure of this $h-\sqrt{3}\times\sqrt{3}$ phase and the role of the domain wall for the surface electronic property.

In this work, we measured the surface-band dispersions and Fermi surfaces before and after the In adsorption on the $\text{Si}(111)\sqrt{3}\times\sqrt{3}\text{-Au}$ surface using angle-resolved photoelectron spectroscopy (ARPES). We found that In adsorbates do not significantly alter the surface-band structure but shift the whole band by 200–500 meV. All the surface-spectral features become very sharp after the In adsorption, which can be understood from the disappearance of the disordered domain-wall network. This electronic structure modification yields a very well-defined 2D electron-gas system with an isotropic Fermi surface filled with 0.3 electrons. The resulting band structure agrees very well with a recent calculation based on the CHCT model [Fig. 1(c)].²⁹ The chemical bondings of the surface atoms were investigated by core-level photoelectron spectroscopy (CLPES) using synchrotron radiation. CLPES spectra indicate that In adsorbates interact mostly with the surface Si atoms. The possible mechanism underlying the present finding is discussed and the role of the domain wall is emphasized.

II. EXPERIMENTAL DETAILS

The photoelectron spectra were measured at beamline 3A2 at Pohang Accelerator Laboratory (Pohang, Korea) and beamline 7 at Advanced Light Source (Berkeley, CA). High-performance hemispherical electron-energy analyzers (R4000, Gamadata Scienta, Sweden) were used at both beam

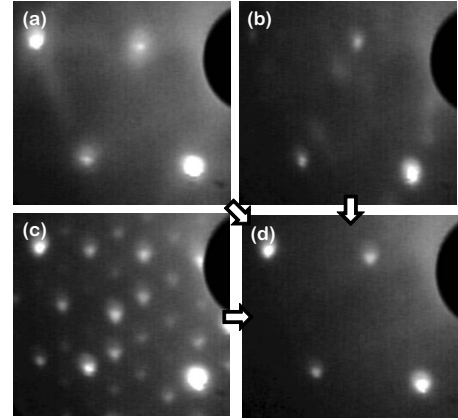


FIG. 2. LEED patterns of the $\text{Au}/\text{Si}(111)$ surfaces with the Au coverage of (a) 0.9 (the $\alpha-\sqrt{3}\times\sqrt{3}$ phase), (b) 1.0 (the $\beta-\sqrt{3}\times\sqrt{3}$ phase), and (c) 1.1 ML (the 6×6 phase). (d) LEED pattern of the same surfaces after the adsorption of In (0.12–0.18 ML) and postannealing at 600 °C.

lines. Band dispersions were measured with the incident beam energy of 45 or 90 eV while Fermi surfaces were mapped with 90 eV photons. All data presented here were obtained at RT. $\text{Si}(111)$ samples cut from an n -doped ($2\sim 8\ \Omega/\text{cm}$) wafer were used. The samples were cleaned *in situ* by direct current heating up to 1230 °C and the clean surfaces were checked by the sharp 7×7 low-energy electron-diffraction (LEED) pattern. Au was evaporated onto the $\text{Si}(111)7\times 7$ surface kept at 600 °C from a tungsten filament source. The postannealing for 4 min at 600 °C followed each Au deposition.

The Au coverage was calibrated with a well-established $\text{Si}(111)5\times 2\text{-Au}$ phase with a nominal coverage of 0.4 ML [1 ML as defined by the surface atomic density of the bulk-terminated $\text{Si}(111)$ surface]. The Au deposition of 0.9 ML resulted in the $\alpha-\sqrt{3}\times\sqrt{3}$ phase as shown in Fig. 2(a). In agreement with the earlier LEED observations,¹³ the $\alpha-\sqrt{3}\times\sqrt{3}$ phase shows cloudlike diffraction streaks in between $\sqrt{3}$ spots. The same annealing procedure with 1.0 ML of Au yielded the $\beta-\sqrt{3}\times\sqrt{3}$ phase shown in Fig. 2(b), which is characterized by the weak and broad ringlike satellite features surrounding $\sqrt{3}$ spots.¹³ The Au deposition of 1.1 ML followed by a slow cooling to RT led to the formation of the 6×6 phase, shown in Fig. 2(c), which exhibits clear fractional-order (1/6) spots due to the ordered domain-wall superstructure.

After Au-induced reconstructions were formed, 0.5 ML of In was deposited by a graphite effusion cell while the samples were held at RT. The coverage of In was referenced by the well-known surface phases of $\text{Si}(111)\sqrt{3}\times\sqrt{3}\text{-In}$, $\sqrt{31}\times\sqrt{31}\text{-In}$, and $4\times 1\text{-In}$, with the nominal coverages of 0.3, 0.5, and 1.0 ML, respectively.³⁰ The postannealing for 5–60 s at 600 °C following the In deposition resulted in 0.06–0.18 ML of In left on the surface, as measured by the In $4d$ photoelectron intensity. In this coverage range, a sharp $\sqrt{3}\times\sqrt{3}$ LEED pattern without any other diffraction features developed as shown in Fig. 2(d), which should correspond to the $h-\sqrt{3}\times\sqrt{3}$ phase without the domain-wall network observed in the previous STM study.²⁷ This procedure was kept

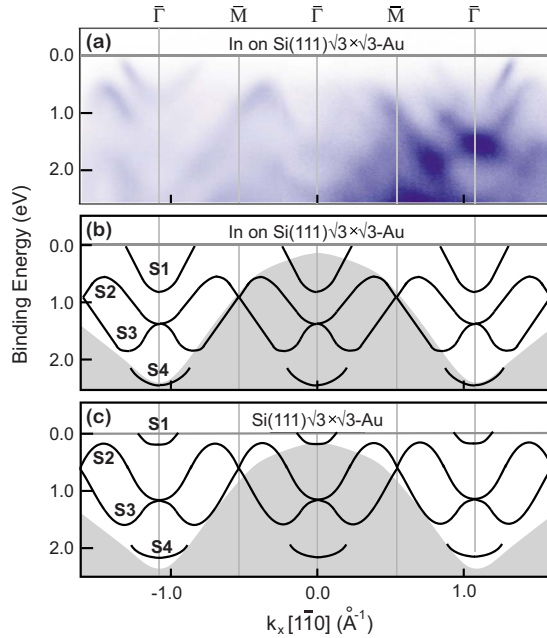


FIG. 3. (Color online) (a) ARPES intensity maps in gray scale (darker contrast for higher intensity) for the In-adsorbed $\text{Si}(111)\sqrt{3}\times\sqrt{3}\text{-Au}$ surface (the $h-\sqrt{3}\times\sqrt{3}$ phase) taken at a photon energy of 45 eV along the $[1\bar{1}0]$ axis (along $\bar{\Gamma}-\bar{M}$ in the surface Brillouin zone). (b) Measured surface-state dispersions by tracing the peak positions of the ARPES spectral features of (a). (c) Similar surface-state dispersions measured for the $\alpha-\sqrt{3}\times\sqrt{3}$ phase before the In adsorption (raw data not shown). The shaded parts in (b) and (c) are the Si bulk band projected on the 1×1 surface Brillouin zone.

consistent with that STM report.²⁷ The sharp $\sqrt{3}\times\sqrt{3}$ LEED pattern was optimized at the In coverage of 0.12–0.18 ML. Below the In coverage of 0.06–0.10 ML, the streaky LEED features of the pristine surface with domain walls were discernible in accord with the STM result²⁷ which showed the mixture of the $h-\sqrt{3}\times\sqrt{3}$ areas with the domain-wall phase. Here, one interesting thing is that the phase transformation by In adsorbates occurred irrespective of the Au coverages from the $\alpha-\sqrt{3}\times\sqrt{3}\text{-Au}$ to $6\times 6\text{-Au}$ phases as shown in Fig. 2.

III. RESULTS AND DISCUSSION

Figure 3(a) shows the band dispersion of the $h-\sqrt{3}\times\sqrt{3}$ surface along the $\bar{\Gamma}-\bar{M}$ direction ($[1\bar{1}0]$) of the $\sqrt{3}\times\sqrt{3}$ surface Brillouin zone. Before and after the In adsorption, the $\alpha-\sqrt{3}\times\sqrt{3}$ surface shows similar dispersions as schematically depicted in Figs. 3(c) and 3(b), respectively. Irrespective of the In adsorption, four surface-state bands can be identified within the bulk band gap, which are fully consistent with the previous reports for the $\alpha-\sqrt{3}\times\sqrt{3}$ surface.^{28,31} The S2 and S3 bands are the most prominent spectral features with strong dispersions. The S4 state is observed only near the edge of the Si bulk band with a largest binding energy. There exists a shallow metallic surface state S1 near the Fermi level.

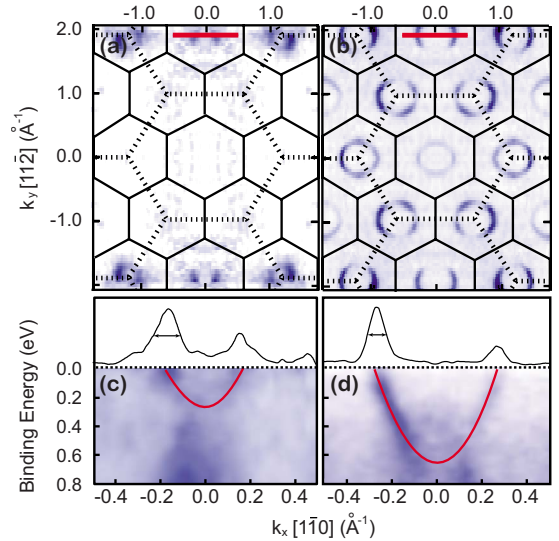


FIG. 4. (Color online) ARPES intensity maps at the Fermi energy to show the Fermi contours of (a) the $\text{Si}(111)\sqrt{3}\times\sqrt{3}\text{-Au}$ surface ($\alpha-\sqrt{3}\times\sqrt{3}$) and (b) the In-adsorbed $\text{Si}(111)\sqrt{3}\times\sqrt{3}\text{-Au}$ surface ($h-\sqrt{3}\times\sqrt{3}$). High photoemission intensity is shown as dark contrast. Surface Brillouin zones for $\text{Si}(111)1\times 1$ structure (dashed lines) and $\text{Si}(111)\sqrt{3}\times\sqrt{3}$ (solid lines) are shown and the energy integration interval of ± 20 meV around E_F was applied. The ARPES intensity maps along k_x (along the $[1\bar{1}0]$ axis), which show the dispersions of the metallic surface state S1 of (c) the $\alpha-\sqrt{3}\times\sqrt{3}$ and (d) $h-\sqrt{3}\times\sqrt{3}$ surfaces. The dispersions were measured along the thick solid lines shown in (a) and (b). The momentum distribution curves of the ARPES intensity at the Fermi level are provided together. All data were obtained with an incident beam energy of 90 eV.

However, a few In-induced changes can be noticed by a closer look. At first, the surface-state spectral features become noticeably sharp after the In adsorption. The comparison of the spectral features, in particular for the S1 surface-state band near the Fermi level, can be found in Figs. 4(c) and 4(d). The sharpening of the spectral features is consistent with the sharpening of the $\sqrt{3}$ LEED spots accompanying the disappearance of the streaky diffraction features due to the domain walls. Thus, this spectral change indirectly indicates that the disordered domain-wall network was removed by the In adsorption and postannealing. The second overall change by the In adsorption is the shift of the whole bands to higher binding energies. This shift is particularly substantial for the metallic S1 band as shown in Figs. 3 and 4; the S1 band shifts by about 500 meV while the S2–S4 bands shift only by 200–300 meV. This shift is not related to the band bending; the band bending shift measured from the Si $2p$ spectra in CLPES and the bulk valence-band features in ARPES is about 60–100 meV in the opposite direction.

The In-induced shift increases substantially the electron filling of the metallic S1 band. Figures 4(a) and 4(b) show the Fermi-surface maps, the intensity maps of photoelectrons from the Fermi level, before and after the In adsorption, respectively. For the pristine $\alpha-\sqrt{3}\times\sqrt{3}$ surface, the Fermi surface consists of a single circle of radius $k=0.16\text{ \AA}^{-1}$, which is in good agreement with the previous study.⁵ Note

that the Fermi circle is not so well defined due to the fuzzy and broad spectral feature of S1. After the In adsorption, the Fermi surface is also composed of a single circle but with a substantially larger radius of $k=0.30 \text{ \AA}^{-1}$. The sharpening of the spectral features, mentioned above, results in a remarkably well-defined Fermi circles. By measuring the area of the Fermi circles, the electron filling of the S1 band is quantified to be 0.3 electrons per unit cell after the In deposition. This is indeed a huge, three times, increase from 0.1 electrons of the pristine surface.

Figures 4(c) and 4(d) are the detailed energy dispersions of the S1 metallic band for both surfaces obtained along the momentum space lines indicated in Figs. 4(a) and 4(b) (thick solid lines). By fitting out the highest intensity positions of the spectra, the band dispersions of the S1 band are more quantitatively obtained. These dispersions are then fitted by parabolic lines as shown in Figs. 4(c) and 4(d).³² The electron-effective mass m^* determined from these fits are the same for both surfaces as $0.3m_e$ within the experimental uncertainty. This evidences that the metallic bands before and after the In adsorption have the same origin. Thus, we conclude that electrons are donated to the S1 band through the In adsorption, directly from In adsorbates themselves or indirectly by the In-induced structural changes.

The In-induced $h-\sqrt{3} \times \sqrt{3}$ surface is optimized at 0.12–0.18 ML as the LEED and the CLPES results tell (the CLPES results are discussed below). If we assume that the electrons are donated from the In adsorbates, then the measured increment in the electron filling corresponds to 0.4–0.6 electrons from each In atom, which is not unusual for a metal adsorbate. The situation is, however, more complicated than the simple electron doping since we did not observe any systematic dependence of the energy shift on the In coverage. The energy shift is consistent for a rather large range of the In coverage, 0.10–0.18 ML, where the $h-\sqrt{3} \times \sqrt{3}$ phase is observed. Below this coverage the ARPES spectral features become fuzzy and the surface changes gradually into the $\alpha-\sqrt{3} \times \sqrt{3}$ phase. Moreover, the energy shifts are largely different for different surface states; two times larger for the S1 band than others. If the energy shift is due to the electron doping, then the change in the chemical potential would shift the whole bands *rigidly*. This manifests that the change in the band structure cannot be explained by the simple electron doping from In adsorbates.

In the well-known case of the Si(111) $\sqrt{3} \times \sqrt{3}$ -Ag surface which has a very similar 2D metallic band, various metallic adsorbates, such as alkali metals, Ag and Au were reported to donate electrons into the 2D metallic band.³³ On the $\sqrt{3} \times \sqrt{3}$ -Ag surface, the amount of the shift or the electron filling depends linearly on the adsorbate coverage to some extent in contrast to the present case. However, this system also shows the deviation from the rigid-shift behavior of the simple electron doping; the metallic surface state exhibits a noticeably larger energy shift than the other fully occupied surface states as in the present case.³³ Although this behavior could be properly reproduced in the recent density-functional theory calculation,³⁴ the underlying mechanism cannot straightforwardly be accounted for from the simple electron-doping picture mainly because the adsorbates interact with

the surface in a complicated way.³⁴

In order to understand the observed electronic structures, we compare the measured band dispersions with those calculated very recently for the structure models of the pristine surface.²⁹ A similar calculation for the In-adsorbed surface is not available at present. The band dispersions are calculated for three structure models of TT, HCT, and CHCT models shown in Figs. 1(a)–1(c).²⁹ As mentioned above, all these models are based on Si and Au trimers. The TT model has both Si and Au trimers rotated slightly from the symmetry lines of the 1×1 structure [Fig. 1(a)]. In the HCT (CHCT) model, Si (Au) trimers are in highly symmetric positions but Au (Si) trimers are rotated [Figs. 1(b) and 1(c)]. The CHCT model was introduced by the early first-principles calculations²⁵ and was supported by the Kikuchi-electron diffraction study.²⁶ The TT model was proposed from the x-ray diffraction result²³ and the HCT model was favored by the recent first-principles calculations.²⁴ In the very recent calculation,²⁹ the total-energy difference between the TT and CHCT models was shown to be marginal while the HCT model was not favored energetically. The close similarity between these structures may prevent an unambiguous determination of the surface structure along with the experimental and theoretical difficulty in dealing with the intrinsic disorder provided by the meandering domain walls.

However, the band dispersions calculated reveal clear distinctions between the models.²⁹ Note that the calculated band dispersions are all shifted by +220 meV to match the experimental data properly. This shift is consistent with the overall shift of the band structure induced by the In adsorption. We especially focus on the shape of the dispersions and the relative binding energies of surface states. While all these models reproduce the four main surface-state bands S1–S4 within the bulk band gap, their detailed dispersions are quite different among the models. Most prominently, the dispersions of S2 and S3 depend largely on the models; they do not cross in the middle of $\bar{\Gamma}-\bar{M}$ only for the CHCT model. One can obviously see that only the CHCT-model calculation reproduces the measured dispersions of the S2, S3, and S4 states properly, which are consistent both for the pristine and In-adsorbed surfaces except for an overall energy shift of 200–300 meV.

As for the metallic S1 state occupied marginally on the pristine surface [solid and dashed line in Fig. 5(d)], the HCT model seems to closely reproduce its dispersion and binding energies, but the CHCT model shows a large discrepancy in the binding energy. This state is due mainly to Au 6s electrons,²⁹ which is similar to the metallic surface state of the Si(111) $\sqrt{3} \times \sqrt{3}$ -Ag surface due to Ag 5s electrons. However, it is remarkable that the CHCT model can properly reproduce this band for the In adsorbed surface, where that band is strongly shifted to a higher binding energy. From this comparison, we can reasonably conclude that the domain-wall-free surface formed after the In adsorption ($h-\sqrt{3} \times \sqrt{3}$) has a well-ordered CHCT structure. On the pristine surface, we suggest that the surface structure must be very close to the CHCT model but is slightly modified. This

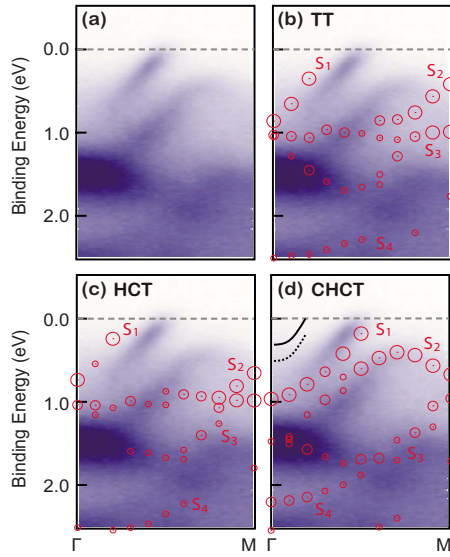


FIG. 5. (Color online) (a) Measured band dispersion of surface states along the $\bar{\Gamma}-\bar{M}$ direction for the In-adsorbed $\text{Si}(111)\sqrt{3} \times \sqrt{3}$ -Au surface (enlarged from Fig. 2). [(b), (c), and (d)] The same data compared with the calculated band dispersions (circles) for TT, HCT, and CHCT models of the ideal $\text{Si}(111)\sqrt{3} \times \sqrt{3}$ -Au surface, respectively (Ref. 29). The calculated dispersions are shifted by +220 meV to match the measured ones properly against the overall shift of the bands induced by the In adsorption. The solid (dashed) line in (d) is the measured dispersion of the S1 state of the $\alpha-\sqrt{3} \times \sqrt{3}$ phase before the In adsorption without (with) the binding energy adjustment of +220 meV.

modification is assumed to be due to the presence of the domain walls. That is, the deviation of the S1 band for the pristine surface from the expectation of the CHCT model could be the effect of the domain-wall network. Within this scenario, the electronic role of In adsorbates is indirect through the removal of the domain walls. This is consistent with the core-level result shown below, which indicates that In adsorbate has marginal chemical interaction with Au. However, even in this case, we have to consider the existence of the electron doping to explain the overall energy shift of the bands, which amounts to 200–300 meV. That is, the change in the electronic structure by the In adsorption is understood as a combined effect due both to the electron doping from the adsorbates and the subtle structural change by the domain-wall removal.

Even within the above explanation, the microscopic interaction of In adsorbates with the surface is uncertain, which can be probed further by CLPES. Figure 6 shows the In 4*d* and Au 4*f* photoelectron spectra for different In coverages on the $\sqrt{3} \times \sqrt{3}$ -Au surface. The In coverage was changed by increasing the postannealing time at 600 °C after the deposition of 0.5 ML of In. From the In 4*d* intensity in Fig. 6(a), the systematic decrease in the In coverage is clear as the postannealing time increases. The clear $\sqrt{3} \times \sqrt{3}$ LEED pattern (the $h-\sqrt{3} \times \sqrt{3}$ phase) was optimized after 5 and 10 s annealings, which correspond to 0.18 and 0.12 ML, respectively. For most of the coverage range where the

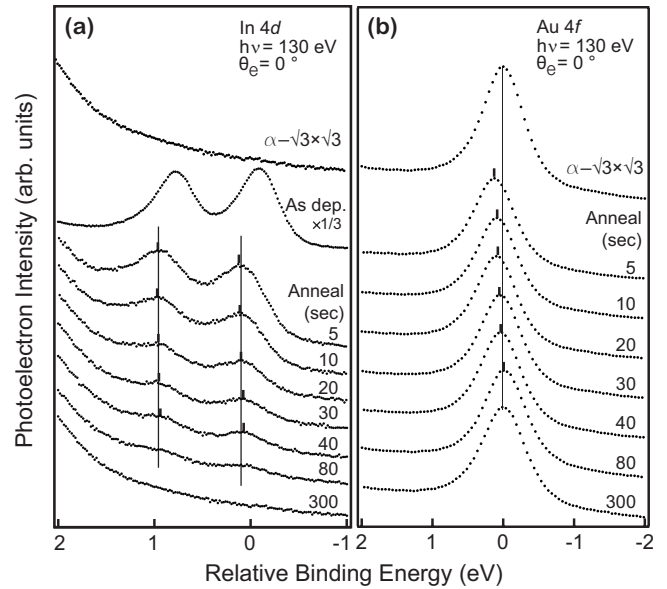


FIG. 6. (a) In 4*d* and (b) Au 4*f* photoelectron spectra of the $\text{Si}(111)\sqrt{3} \times \sqrt{3}$ -Au surface before the In adsorption (top) and after the In deposition of 0.5 ML at 600 °C with subsequent annealings at 600 °C for the durations given. The In 4*d* spectrum for the as-deposited surface without an annealing is also given as scaled by 1/3. All spectra were obtained with a photon energy of 130 eV at the normal-emission geometry. The band banding shifts were corrected as referenced by the Si 2*p* bulk component.

$h-\sqrt{3} \times \sqrt{3}$ phase is formed (up to 40 s postannealing) the In 4*d* spectra show no significant change of the binding energy. Moreover, within this coverage range, the In 4*d* spectral shape can be consistently fitted with a single spin-orbit doublet indicating the largely unique bonding configuration or the unique adsorption site of In on this surface.

As shown in Fig. 6(b), In adsorbates do not cause a significant change in the Au 4*f* spectra. This indicates that In adsorbates do not chemically interact with Au atoms. Only a marginal energy shift, up to 80 meV, is observed for the Au 4*f* peak between the pristine and the In-induced surface. The higher binding-energy shift is not consistent with the increase in the metallic electron density on the Au sites implying again that the electronic change in the surface has a complicated mechanism. The direct electron doping from In adsorbates into the Au 6*s* state (S1) cannot fully explain the present observation.

In contrast, In adsorbates induce a noticeable change in the Si 2*p* spectra (see Fig. 7). While the Si 2*p* spectra for the pristine surface is fully consistent with the previous report,¹³ those for the optimized $h-\sqrt{3} \times \sqrt{3}$ surface (at 5 and 10 s postannealings) are distinct with a prominent surface-related component at the higher binding-energy side (see the dashed lines). The surface sensitivity of this component was indicated by the emission-angle dependence of its intensity. As the In coverage decreases below 0.12 ML (for the postannealings longer than 20 s), the Si 2*p* spectra gradually return to those of the pristine surface. This clearly shows that the desorption of In gradually recovers the $\alpha-\sqrt{3} \times \sqrt{3}$ surface with domain walls. This result is consistent with the recent STM study, which showed the mixture of the homogeneous

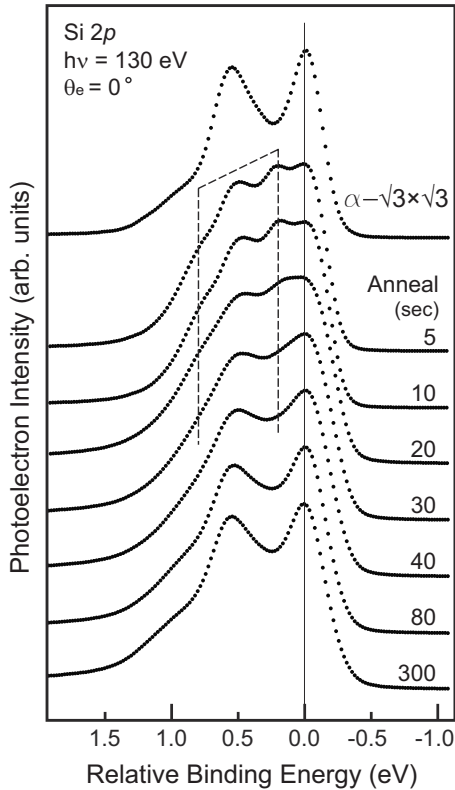


FIG. 7. Si 2*p* spectra of the pristine Si(111) $\sqrt{3}\times\sqrt{3}$ -Au surface (the top spectrum) and of the surfaces for the postannealing series after the In deposition of 0.5 ML at 600 °C. All spectra were obtained with a photon energy of 130 eV at the normal emission geometry.

and $\alpha-\sqrt{3}\times\sqrt{3}$ surfaces for a smaller In coverage than the optimum value.²⁷ On the other hand, Si 2*p* spectra tell that the In adsorbates interact directly with the surface Si atoms in contrast to Au atoms. It is highly likely that the In atoms adsorb in the middle of the Si trimers as suggested by the STM study²⁷ [Fig. 1(d)]; the In atoms could not be probed at all at room temperature due probably to their active diffusion but could be imaged at low temperature. A more detailed curve-fitting analysis of Si 2*p* for the In-adsorbed surfaces was not successful with a large uncertainty of the fitting due mainly to the broad-line shape for the optimized $h-\sqrt{3}\times\sqrt{3}$ surface and the intrinsically complicated line shape with many different surface components for the $\sqrt{3}\times\sqrt{3}$ surface itself.¹³

As discussed above, most of the spectral information is not consistent with the simple electron doping from the In adsorbates into the surface metallic state of the Au 6*s* electrons. Moreover, the change in the band structure does not scale with the In coverage but is consistent with the change in the LEED pattern. These results indicate that the change in the band structure is at least partly related to the domain walls or the structural changes. This is also consistent with the fact that the band structure of the pristine $\sqrt{3}\times\sqrt{3}$ -Au surface itself, especially the metallic surface state S1, depends strongly on the change in the domain-wall density for

different Au coverages. A substantial structural modification by the In adsorbates is not likely from the ARPES result. Since the domain wall is generally caused by the surface strain, one can suggest that the change in the surface strain within the $\sqrt{3}\times\sqrt{3}$ domains results in the change in the electron filling of the S1 state. The electronic role of In adsorbates in this case is indirect, that is, to change the surface strain through the bonding with the Si surface atoms. However, as mentioned above, the overall shift of the band dispersions (about 200–300 meV) should come from the doping from the adsorbates. The doping is a nonlocal phenomenon and is not contradictory to the absence of the local chemical interaction between In and Au. Further theoretically study is required in order to clarify the adsorption structure of In atoms and to check the effect of In adsorbates on the surface strain field and the effect of the strain on the surface band dispersion.

The temperature dependence of the band structure would also be interesting since the previous STM result²⁷ suggested that In adsorbates migrate actively at RT. We have measured the whole band dispersions and Fermi surfaces from RT down to 40 K but could not find any substantial change. This indicates that the local adsorption site of In adsorbates is consistent over this temperature range. This finding seems also qualitatively consistent with the nonlocal and indirect interaction of In adsorbates with the surface band structure.

IV. SUMMARY

Using valence-band and core-level photoelectron spectroscopy, we have studied the effect of the In adsorption on the 2D metallic band structure of the $\sqrt{3}\times\sqrt{3}$ phases of Au on the Si(111) surface. In agreement with the previous STM result²⁷ showing that the In adsorption removes the intrinsic domain-wall network of the $\sqrt{3}\times\sqrt{3}$ -Au surface, LEED shows a very sharp $\sqrt{3}\times\sqrt{3}$ pattern with no streaky feature from domain walls. The band structure exhibits distinct changes accompanying the disappearance of domain walls; the whole bands shift by 200–300 meV to higher binding energy and the whole spectral features get significantly sharp. Moreover the electron filling of the metallic surface states increases substantially with a larger energy shift of 500 meV. The resulting Fermi surface is isotropic with an electron filling of 0.3 electrons and an effective mass of $0.3m_e$. That is, the In-adsorbed $\sqrt{3}\times\sqrt{3}$ surface forms an ideal 2D electron-gas system. This band structure agrees well with the theoretical expectation²⁹ for the ideal $\sqrt{3}\times\sqrt{3}$ -Au structure based on the CHCT model without any In adsorbates. The core-level spectra show that the In adsorbates interact not with the Au atoms but with Si surface atoms. This is consistent with the adsorption site of In on the Si trimers, which was suggested by the STM study.²⁷ We suggest that the band-structure changes, the overall energy shift and the enhanced electron filling (or stabilization) of the metallic state,

are due to the electron doping by the adsorbate and to the disappearance of the domain walls (the change in the surface strain), respectively. The role of In adsorbates are understood to be twofold; directly doping electrons and indirectly changing the surface strain by the bonding with the Si surface atoms. Further theoretical study is required to understand the microscopic mechanism of the domain wall in determining the surface-band structure.

ACKNOWLEDGMENTS

This work was supported by MOST through Center for Atomic Wires and Layers of the CRi program. J.K.K. and K.S.K. were partly supported by the BK 21 program. HWY is grateful to M. H. Kang for enlightening discussion and encouragement.

*Author to whom all correspondence should be addressed; yeom@yonsei.ac.kr

- ¹H. H. Weitering, J. Chen, N. J. DiNardo, and E. W. Plummer, *Phys. Rev. B* **48**, 8119 (1993).
- ²J. M. Carpinelli, H. H. Weitering, M. Bartkowiak, R. Stumpf, and E. W. Plummer, *Phys. Rev. Lett.* **79**, 2859 (1997).
- ³S. C. Erwin and H. H. Weitering, *Phys. Rev. Lett.* **81**, 2296 (1998).
- ⁴G. Santoro, S. Scandolo, and Erio Tosatti, *Phys. Rev. B* **59**, 1891 (1999).
- ⁵J. N. Crain, K. N. Altmann, C. Bromberger, and F. J. Himpsel, *Phys. Rev. B* **66**, 205302 (2002).
- ⁶I. Matsuda, T. Hirahara, M. Konishi, C. Liu, H. Morikawa, M. D'angelo, S. Hasegawa, T. Okuda, and T. Kinoshita, *Phys. Rev. B* **71**, 235315 (2005).
- ⁷E. Rotenberg, H. Koh, K. Rossnagel, H. W. Yeom, J. Schäfer, B. Krenzer, M. P. Rocha, and S. D. Kevan, *Phys. Rev. Lett.* **91**, 246404 (2003).
- ⁸R. Cortés, A. Tejada, J. Lobo, C. Didiot, B. Kierren, D. Malterre, E. G. Michel, and A. Mascaraque, *Phys. Rev. Lett.* **96**, 126103 (2006).
- ⁹W. H. Choi, H. Koh, E. Rotenberg, and H. W. Yeom, *Phys. Rev. B* **75**, 075329 (2007).
- ¹⁰H. W. Yeom, S. Takeda, E. Rotenberg, I. Matsuda, K. Horikoshi, J. Schaefer, C. M. Lee, S. D. Kevan, T. Ohta, T. Nagao, and S. Hasegawa, *Phys. Rev. Lett.* **82**, 4898 (1999).
- ¹¹J. L. McChesney, J. N. Crain, V. Pérez-Dieste, F. Zheng, M. C. Gallagher, M. Bissen, C. Gundelach, and F. J. Himpsel, *Phys. Rev. B* **70**, 195430 (2004).
- ¹²W. H. Choi, P. G. Kang, K. D. Ryang, and H. W. Yeom, *Phys. Rev. Lett.* **100**, 126801 (2008).
- ¹³H. M. Zhang, T. Balasubramanian, and R. I. G. Uhrberg, *Phys. Rev. B* **65**, 035314 (2001).
- ¹⁴T. Nagao, S. Hasegawa, K. Tsuchie, S. Ino, C. Voges, G. Klos, H. Pfnur, and M. Henzler, *Phys. Rev. B* **57**, 10100 (1998).
- ¹⁵M. Hupalo, J. Schmalian, and M. C. Tringides, *Phys. Rev. Lett.* **90**, 216106 (2003).
- ¹⁶M. Yakes, V. Yeh, M. Hupalo, and M. C. Tringides, *Phys. Rev. B* **69**, 224103 (2004).
- ¹⁷J. Falta, A. Hille, D. Novikov, G. Materlik, L. Seehofer, G. Falk-

enberg, and R. L. Johnson, *Surf. Sci.* **330**, L673 (1995).

- ¹⁸D. Grozea, E. Bengu, and L. D. Marks, *Surf. Sci.* **461**, 23 (2000).
- ¹⁹L. D. Marks, D. Grozea, R. Feidenhansl, M. Nielsen, and R. L. Johnson, *Surf. Rev. Lett.* **5**, 459 (1998).
- ²⁰J. Nogami, A. A. Baski, and C. F. Quate, *Phys. Rev. Lett.* **65**, 1611 (1990).
- ²¹E. A. Khramtsova and A. Ichimiya, *Phys. Rev. B* **57**, 10049 (1998).
- ²²H. Aizawa, M. Tsukada, N. Sato, and S. Hasegawa, *Surf. Sci. Lett.* **429**, L509 (1999).
- ²³A. Saito, K. Izumi, T. Takahashi, and S. Kikuta, *Phys. Rev. B* **58**, 3541 (1998).
- ²⁴T. Kadohira, J. Nakamura, and S. Watanabe, *e-J. Surf. Sci. Nanotechnol.* **2**, 146 (2004).
- ²⁵Y. G. Ding, C. T. Chan, and K. M. Ho, *Surf. Sci.* **275**, L691 (1992).
- ²⁶I. H. Hong, D. K. Liao, Y. C. Chou, C. M. Wei, and S. Y. Tong, *Phys. Rev. B* **54**, 4762 (1996).
- ²⁷D. V. Gruznev, I. N. Filippov, D. A. Olyanich, D. N. Chubenko, I. A. Kuyanov, A. A. Saranin, A. V. Zotov, and V. G. Lifshits, *Phys. Rev. B* **73**, 115335 (2006).
- ²⁸H. M. Zhang, T. Balasubramanian, and R. I. G. Uhrberg, *Phys. Rev. B* **66**, 165402 (2002).
- ²⁹J. Y. Lee and M. H. Kang, *J. Korean Phys. Soc.* **53**, 3671 (2008); J. Y. Lee and M. H. Kang (unpublished).
- ³⁰M. Kawaji, S. Baba, and A. Kinbara, *Appl. Phys. Lett.* **34**, 748 (1979).
- ³¹K. N. Altmann, J. N. Crain, A. Kirakosian, J.-L. Lin, D. Y. Petrovykh, F. J. Himpsel, and R. Losio, *Phys. Rev. B* **64**, 035406 (2001).
- ³²The measured band dispersions deviate from the parabolic fit at the bottom (the high binding energy) to become more linear dispersions. We focus on the effective mass of electrons near the Fermi level.
- ³³J. N. Crain, M. C. Gallagher, J. L. McChesney, M. Bissen, and F. J. Himpsel, *Phys. Rev. B* **72**, 045312 (2005).
- ³⁴H. J. Jeong, H. W. Yeom, and S. Jeong, *Phys. Rev. B* **77**, 235425 (2008).